

Accepted for publication in Textile Research Journal

Published in 2013

DOI: 10.1177/0040517513478455

A comparative analysis of hollow and solid glass fibers

Sándor KLING¹, Tibor CZIGÁNY^{1,2*}

¹Department of Polymer Engineering, Faculty of Mechanical Engineering,
Budapest University of Technology and Economics,
H-1111 Budapest, Műegyetem rkp. 3., Hungary

²MTA–BME Research Group for Composite Science and Technology,
H-1111 Budapest, Műegyetem rkp. 3., Hungary

*corresponding author: czigany@eik.bme.hu

Abstract

Comparative analyses have been completed on hollow and solid E-type glass fibers. Single fiber tensile tests were performed and correlations have been determined between the geometry and the tensile strength of the fibers. The flexural properties of the solid and the hollow fibers have been determined with deflection tests. The hollow glass fibers showed higher tensile strength and flexural rigidity than the solid glass fibers in the case of similar outer diameter. The hollow fibers were filled with the help of capillary effect, and the filling process was examined as a function of the viscosity and the contact angle between glass and fluids. Relationship has been detected between fiber filling speed and the inner diameter of the fibers, and the filling speed was increased by the lower viscosity and contact angle.

Keywords

Hollow glass fiber, fiber tensile strength, fiber flexibility, filling by capillary effect

Introduction

The use of fiber reinforced polymer composites increases rapidly thanks to the innovation of the material and the geometry of the fibers. The most frequently used fibers are glass, carbon and aramid fibers, but the use of basalt, flax, hemp and thermoplastic fibers also increases significantly [1-3]. Beside the development of the fiber material many researchers have been

working on optimising the cross section shape [4-6]. Kim and Park [7] compared concrete reinforced by C-shaped, solid and hollow carbon fiber. They showed that C-shape carbon fiber reinforced concrete has 40% higher tension and bending stiffness, than the ones reinforced by solid or hollow carbon fiber. They explained the better properties in case of the C-shape cross sectional reinforcement by the bigger linking surface to the matrix. Park *et al.* [8] analysed the reinforcement effect of the conventional solid, C-shaped, and hollow fibers in epoxy matrix. The C-shaped fiber was shown to provide 40-50% higher mechanical properties, greater damping factor than those provided by the solid or hollow reinforcing fibers. These were explained by the high surface to volume ratio, which means larger contact area between the reinforcing fiber and the matrix. Beyerlein *et al.* [9] applied bond shaped fibers to prevent fiber pulling out, and the fiber length, the size and shape of fiber ends were optimised. By the effect of bigger fiber ends the toughness of composites can be improved, since fiber pulling out happens at a higher load. Bond *et al.* [10] compared glass fibers with triangular and circular cross sections by single fiber tensile tests. It was shown that tensile strength of triangular glass fibers is higher by 25% than that of the conventional circular glass fibers. Compression tests were performed on micro composite specimens reinforced by 12-15 filaments, and triangular fiber reinforcement ensured 60% higher compression strength than conventional fiber reinforcement, which was explained by the fact that the triangular fibers could not be packed tightly and hence resulting in higher moment of inertia. Mechanical tests were performed on composite specimens, and the composites reinforced by triangular fibers showed 20% higher tensile strength, 40% higher compressional strength and 5% higher interlaminar strength than the conventional circular fiber reinforced composites.

Among the novel fiber geometries the spreading of hollow fibers is the most notable due to the more advantageous mechanical properties than the conventional fibers [11], and the storing function [12]. There are some patents in the literature on the hollow fiber standardised manufacturing methods [13-15]. Hucker *et al.* [16] fabricated solid and hollow glass fibers from glass preforms under laboratory conditions and examined the effects of the manufacturing conditions on the tensile strength. The material composition of the solid and hollow preform was the same with a minimal difference. Tensile strength of solid fibers decreased with increasing fiber diameter. The strength of the solid fibers decreased with decreasing drawing speed and increased with temperature. Higher strength could be reached in case of the hollow fibers by increasing the drawing tension, namely the feeding of the preform was decelerated as much as possible, the viscosity of the drawn glass was increased by decreasing the furnace temperature and the drawing speed was set to the minimum. It was

shown that the tensile strength could be increased by increasing the ratio of the inner and the outer diameter of the fibers.

Beside the advantageous mechanical properties the hollow fibers could be used as a membrane [17, 18], together with stored liquids in composites. Fibers could be filled by indicator liquids which would flow onto the surface after cracking, thus the condition of the structure could be checked easily [19, 20]. Hollow fibers could also be filled by a healing agent, and after the breakage of the fiber this liquid could flow into the crack and this could stop the propagation of the crack by cross linking there [21-23].

The aim of this article is to compare the mechanical properties of the solid and hollow glass fibers. The analysis of the hollow fiber filling ability is demonstrated with different viscosity liquids and the influence of the viscosity and contact angle on the filling speed is also shown. The goal of this study was to learn the effect of the hollowness of the hollow fibers on the mechanical properties and the filling ability of them, because they could be used for weight reduction on composite structures or for self-repairing composites.

Materials and test methods

Fibers

The hollow fibers were purchased from R&G Faserverbundwerkstoffe GmbH (Germany), the diameter of which was nominally 10-12 μm . Solid fibers were provided by 3b Fiberglass (Belgium) with a nominal diameter of 10 μm .

The accurate chemical composition was defined with inductively coupled plasma optical emission spectrometry (ICP-OES) method and it was established that among the components there wasn't significant difference, the main components are 60% SiO_2 , 23% CaO , 11% Al_2O_3 and 6% others.

Determination of the fiber's diameter and the tensile strength. The measurement of the diameter of the single filaments and the test specimens was executed with an Olympus BX 51M (Japan) optical microscope with 50x magnification illuminated from below. Photographs were prepared with a C-5060 CAMEDIA type digital camera, and the fiber diameter measurement was done with AnalySIS image processor software. Every test specimen was measured at three places equally divided along the fiber length. Both the internal and external diameter of the hollow fibers could be measured when focusing right onto the middle of the fiber cross section.

The fiber tensile tests were executed according to the EN ISO 5079 [24] standard, on 100 pieces of each fiber type with a 25 mm clamping length. The tests were performed using a Zwick Z005 universal tester at a speed of 2 mm/min. As the fiber diameters are known, supposing a circular fiber cross section at all fibers, the cross sectional area could be calculated. Reading the fiber tension force (F_{ft}) the fiber tensile strength (σ_{ft}) could be calculated, and on the basis of the breaking elongation the breaking strain was calculated. The Young modulus (E_f) was calculated from the gradient of the tensile curve on the 0.05 and 0.25% relative strain interval.

Determination of fiber deflection. The fiber flexibility could be characterized by the measurement of the fiber deflection. A 50 mm long fiber was clamped in front of a measuring rod (Figure 1) and the so clamped fiber was put into a glass box, which is free from all air motion, to help determining the value of the deflection.

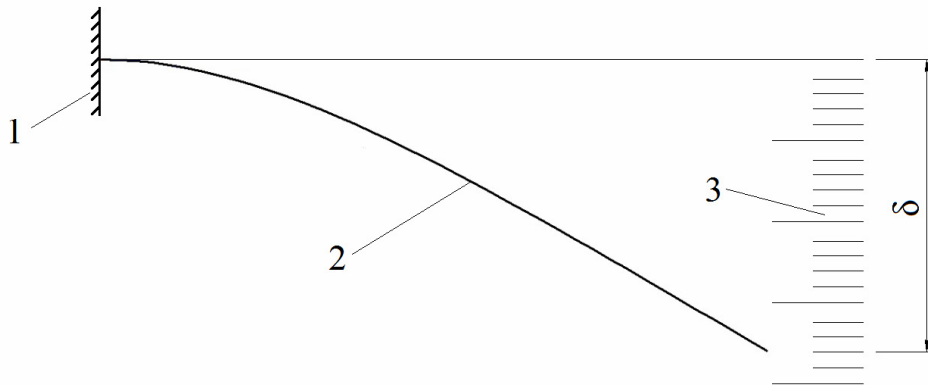


Figure 1. Arrangement of the fiber deflection measurement. 1 – clamping; 2 – fiber; 3 – measuring rod. (single cantilever setup)

The Young modulus could not be calculated by the simple fiber end displacement, because in consequence of the extensive flexural deflection the loading becomes nonlinear. There are several methods to calculate large deflection of a beam [25], and we used the one defined by Holden [26]. The equation of Holden is for a nonlinear, extensive bending deflection for a beam which is loaded along the length and clamped fixed on one end is seen in Equation 1:

$$k = \frac{w \cdot L^3}{D} \quad (1)$$

If the length of the fiber (L (mm)), the rate of the deflection (δ (mm)) and the value of the load (w (N/m)) was known, then the flexural rigidity (D (Nm²)) of the fiber could be defined. The value of „ k ” was defined by the ratio of δ/L and a $k(\delta/L)$ curve that was suggested by Holden [26]. The fibers were fixed with a tape on a horizontal surface, and the length of the fiber was always set to 50 mm. The fiber deflection was determined with the aid of the measuring rod as it is seen in Figure 1, thus the value of „ k ” could be defined. Every fiber diameter was measured at 3 points, and the cross sectional area was calculated by the average diameter, then the fiber mass was determined by the density of glass, which was considered for this single cantilever flexure. The bending elasticity modulus can be calculated by Equation 2:

$$E_{fb} = \frac{D}{I} \quad (2)$$

where E_{fb} is the fiber flexural modulus, I is the moment of inertia. The calculation method defined by Holden corresponding with the Euler-Bernoulli beam theory [26].

Filling of the hollow fibers with resin

Hollow fibers were filled with different resin components and hardeners. The fibers were laid onto a glass plate scratched in every 10 mm, and the fibers were cut at the 0 and the 50 mm line (demonstrated later). The glass plate was placed under an Olympus BX 51M optical microscope (Japan) with the fiber on it, and a resin drop was placed to the end of the fiber. The fibers began to suck the resin by the capillary action and after every 10 mm the time passed was recorded since the dropping. The temperature of the measurement was 23°C.

Different laminating and injecting resins were used for fiber filling. Different resin systems were chosen in order to examine the affecting action of the viscosity. The properties of the resin systems are seen in Table 1

Resin component (A)	Curing agent (B)	Mixing ratio A:B	Potlife (min)
Ipox MS90 A	Ipox MS90 B	100:33	570
Ciba LY 5082	Ciba HY 5083	100:23	100

Eporezit AH12	Eporezit T58	100:40	100
---------------	--------------	--------	-----

Table 1. Applied resin systems

The measurement of the dynamic viscosity was executed with an AR2000ex rheometer (USA). Resin film was placed between a rotating and a fixed plate, and the dynamical viscosity was defined by the rotating resistance. The measurement was completed at a constant temperature of 23°C.

The contact angle was defined by the help of a Ramé-Hart NRL C.A. 100 goniometer (USA) at room temperature (23°C). A resin drop was placed onto a glass plate having chemical components corresponding to the components of the glass fibers. The contact angle could be read with the help of scale by focusing on the edge of the resin drop by a microscope. Averaging the results of the measurements of each liquid the mean contact angle between the glass plate and the liquid was given. Before each measurement the glass plates were cleaned with acetone.

The shear rate of the streaming ideal liquids was calculated by the reordered Hagen–Poiseuille Equation 3 [27]:

$$\gamma = \frac{8v}{d_i} \quad (3)$$

where γ is the shear rate, v is the speed of the liquid front, d_i is the internal diameter of the hollow fiber.

Results and discussion

Fiber tensile test

For better understanding, the fiber cross-sectional filling factor (FCF) was adopted, which indicates the cross sectional area surface ratio of the hollow fiber (Equation 4).

$$FCF = \frac{A_o - A_i}{A_o} = \frac{d_o^2 - d_i^2}{d_o^2} \quad (4)$$

where A_o is the cross sectional area calculated by the outer diameter, A_i is the cross sectional area of the hollow, d_o is the outer diameter, and d_i is the internal diameter.

The geometrical and fiber tension examinations were executed as it is written in chapter Materials and test methods. The tensile strength distribution of the fibers was described by the two-parameter Weibull [28] distribution (Equation 5).

$$F(\sigma_{fi}) = 1 - \exp\left(-\left(\frac{\sigma_{fi}}{a_w}\right)^{b_w}\right) \quad (5)$$

where a_w is the scale factor (Weibull stiffness), and b_w is the Weibull modulus. The tensile strength values were ordered to increasing sequence, and the row number (i) of the so ordered stiffness was divided by the number of all measurements (n). The points calculated so were plotted creating an empirical distribution function and curve was fitted on by Equation 5 (Figure 2).

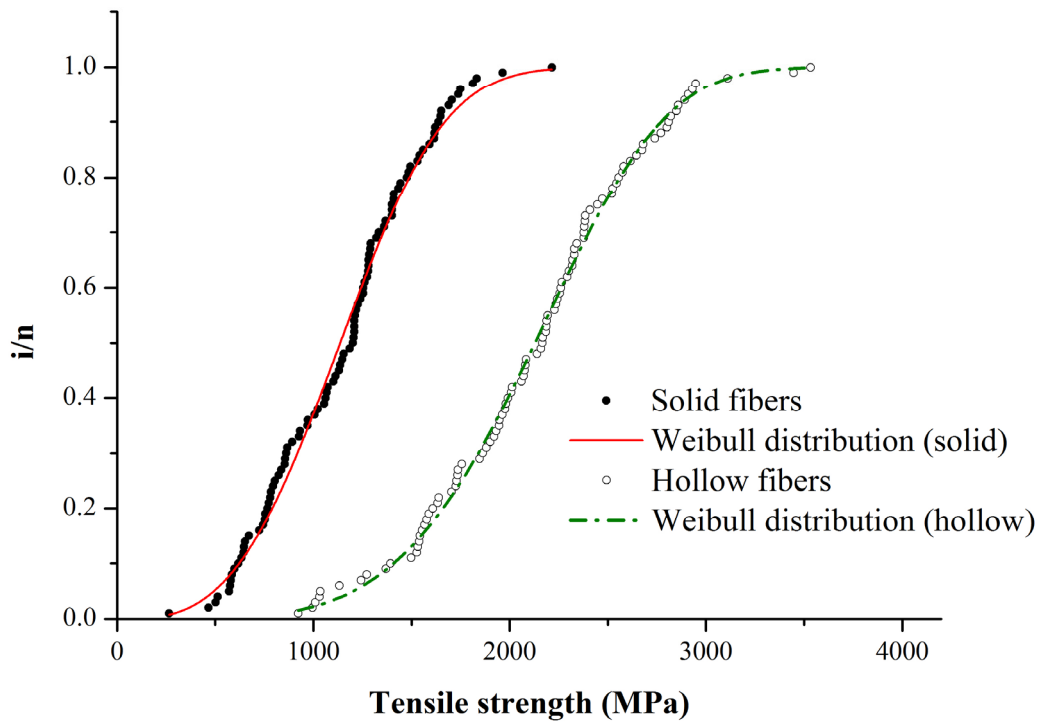


Figure 2. The distribution function of the tensile tests of solid and hollow fibers

The correlation coefficient of the fittings is 0.99 in the case of both the hollow and the solid fibers, which is an acceptable accurate fitting. The results are seen in Table 2.

	Diameter (μm)	FCF (-)	Tensile force (N)	Tensile strength (MPa)	Young modulus (GPa)	Weibull strength parameter (MPa)	Weibull modulus parameter (-)
Solid fibers	12.82 \pm 0.90	1	0.165 \pm 0.0315	1091.1 \pm 345.5	44.96 \pm 4.19	1278.13	3.12
Hollow fibers	12.10 \pm 1.78	0.625 \pm 0.093	0.136 \pm 0.0336	2129.6 \pm 561.2	73.83 \pm 16.48	2307.23	4.55

Table 2. The mean values and the empirical standard deviation of the fiber parameters and the tensile strength properties

While the parameters of the distribution function are known, the expected value ($E(\sigma_{fi})$) and the standard deviation ($V(\sigma_{fi})$) of tensile strength determined by the fitted Weibull distribution could be calculated by Equations 6 and 7:

$$E(\sigma_{fi}) = a_w \cdot \Gamma\left(1 + \frac{1}{b_w}\right) \quad (6)$$

$$V(\sigma_{fi}) = a_w \sqrt{\Gamma\left(1 + \frac{2}{b_w}\right) - \Gamma^2\left(1 + \frac{1}{b_w}\right)} \quad (7)$$

The results of the calculations are seen in Table 3.

	Tensile strength (MPa)	
	Expected value	Standard deviation
Solid fibers	1143	401
Hollow fibers	2107	525

Table 3. The expected value and standard deviation of the tensile strength of each fiber defined by Weibull distribution factors

The breaking force of the hollow fibers is smaller than the one of the solid fibers, but the tensile strength is higher by 95%. There are more reasons of it. In the case of smaller wall thickness there are less defects in the cross section, which means higher strength and elastic

modulus. The smaller thickness means also the higher orientation of the molecular chains [29], which also increases the mechanical properties. The tensile strength is plotted as a function of the FCF, and trend line fitted onto the points, it is seen that in the examined region the fiber tensile strength increases with decreasing FCF (Figure 3).

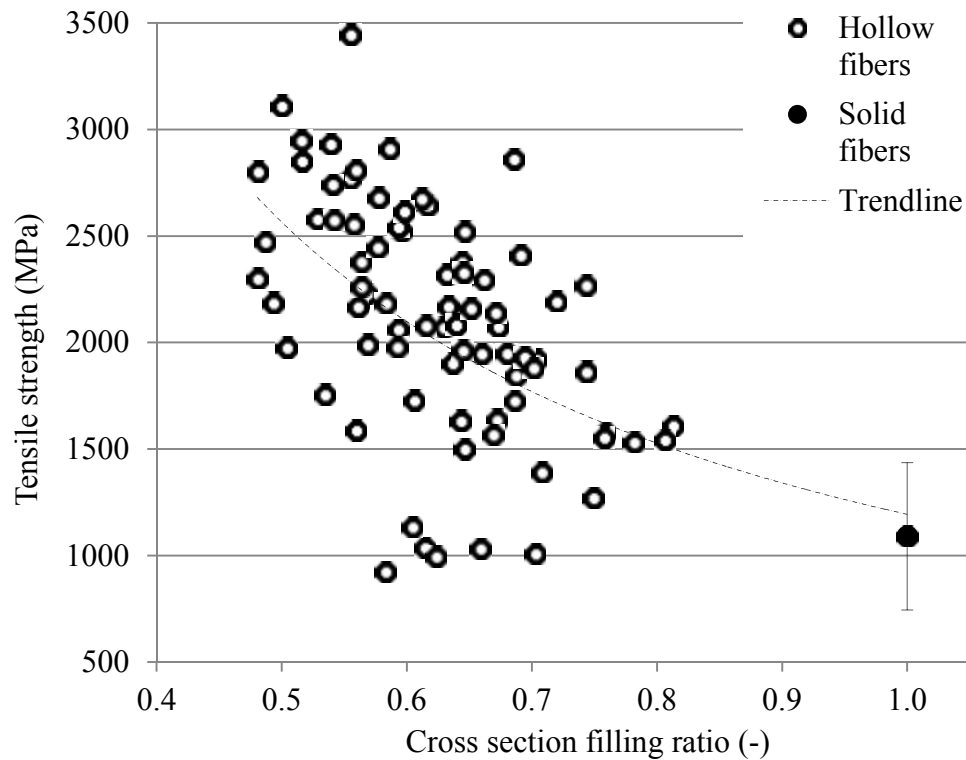


Figure 3. Tensile strength as a function of FCF.

The solid circle shows the mean tensile strength and the scatter of the solid fibers. The decreasing FCF means smaller wall thickness of the fiber, which causes higher strength and elastic modulus, as it is well seen with the aid of the trend line.

Fiber flexibility analysis

The holes of the hollow fibers are not concentric with the outer diameter, which causes inaccuracy when measuring fiber deflection. The SEM shot on the polished surface of fiber cross sections embedded into resin can be seen in Figure 4.

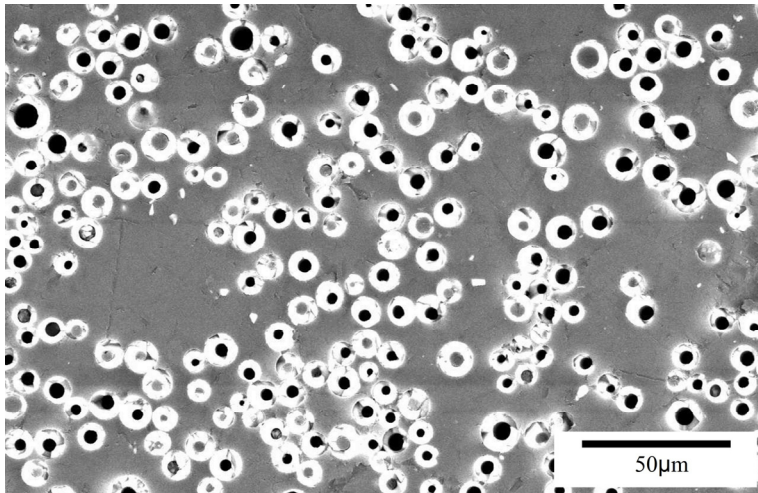


Figure 4. SEM shot on the polished surface of the fiber cross section embedded into resin.

The outer and the internal diameters of the fibers were defined before the determination of fiber deflection with optical microscope, which is not able to detect the portion of the eccentricity. If the eccentricity would be known, the fixing position of the fiber on the surface would still be unknown, so the accuracy of the measurement is bound to happen. The degree of the inaccuracy depends on the portion of the eccentricity and on the fixing position. The extreme positions of the eccentricity can be seen in Figure 5.

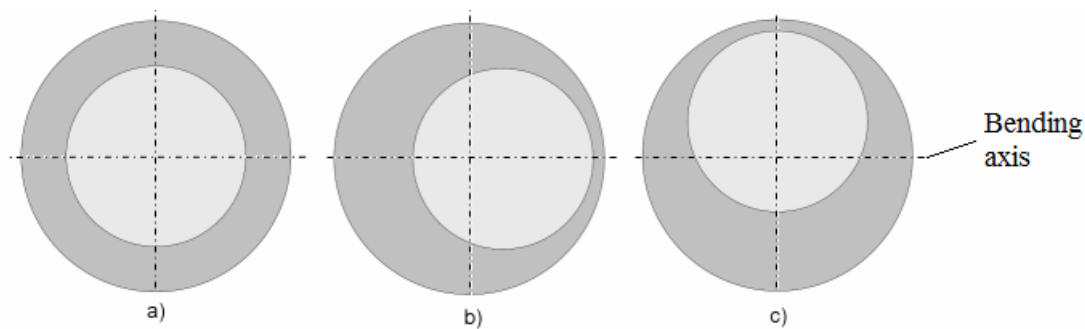


Figure 5. a: concentric hollow fiber, b-c: eccentric hollow fiber in extreme positions.

On Figure 5(a) is the ideal, when the moment of inertia of the fibers can be counted precisely. Figure 5(b) does not affect much the moment of inertia on the bending axis, while it causes a little twisting moment during the fiber deflection, but it does not bring about significant error. Figure 5(c) is the most critical, that can cause a 75% overestimation the moment of inertia in an extreme instance (12 μm outer diameter, 8 μm internal diameter and 3.5 μm eccentricity in vertical direction).

Fiber deflection determinations have been executed in order to compare the flexibility properties of the fibers as it is written in Materials and test methods. The fiber deflection analysis has been performed on 50 solid fibers and on 75 hollow fibers (Table 4).

	Deflection (mm)	E_{fb} (GPa)
Solid fibers	25.48±3.21	60.35±12.05
Hollow fibers	16.95±6.21	88.10±38.08

Table 4. Fiber deflections and bending elasticity modulus

As the tensile strength was affected by FCF, the fiber deflection was also affected by it in a positive direction. In Table 4 it is seen that the hollow fibers have 33% smaller deflection, and 45% higher fiber flexural modulus, which was calculated by Equation 2. The ratio of the moment of inertia and the mass is bigger at hollow fibers caused by the geometry. Calculating the moment of inertia the diameters are on the fourth power, while calculating the cross sectional area they are on the second power. This ratio is the biggest at 0.5 FCF, in other words when the mass is the half of the solid fiber, the moment of inertia is 75% of the solid fiber in case of concentric hollow fiber.

Filling the hollow fibers with liquids

Hollow fibers were filled with liquids, and the affecting factors were examined. The resin components were pigmented for better visibility (good tracking) with Eporezit SZPM black dye, and the curing agents were coloured with an iron oxide based powder pigment.

The contact angle between glass and the resins, the dynamic viscosity of the resins, the fiber filling speed by capillary action were analysed, and the correlation between them were explored. Three type of epoxy resin component and the belonging curing agents were used for the measurements.

The dynamic viscosity was measured with and without pigmentation of the resin components and curing agents as it is written in Materials and test methods. The viscosity of the liquids was increased by the dyes, so the filling process could be examined with liquids of different viscosities.

The contact angle between glass and liquids was measured as it is written in Materials and test methods. The results and their scatter are shown in Figure 6.

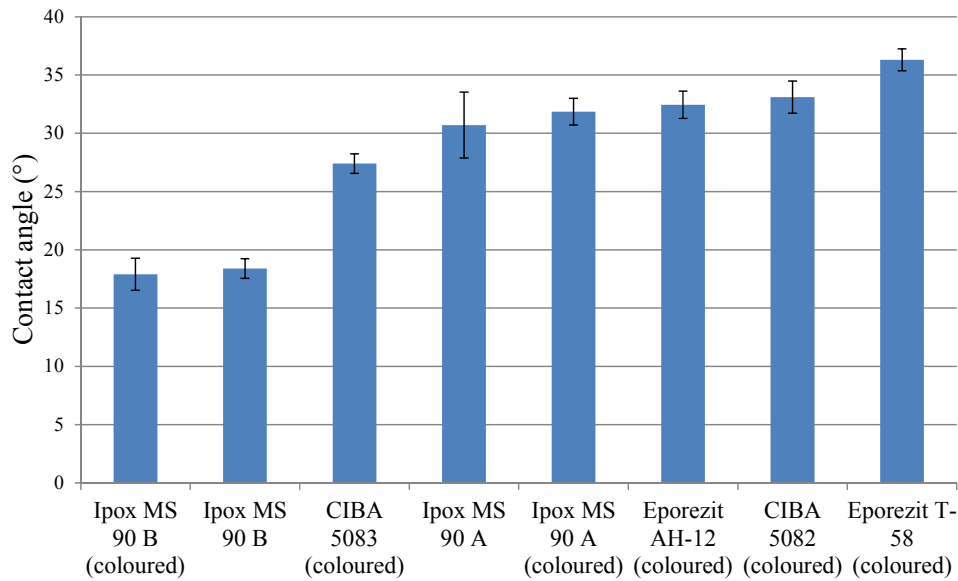


Figure 6. Contact angle between glass plate and liquids

All the liquids were pigmented, and Ipox MS 90A resin component and Ipox MS 90B curing agent was examined also in an uncoloured condition. Since there was no significant difference between the coloured and the uncoloured liquids, the contact angle measurement of the other uncoloured liquid types was skipped. The differences between the contact angle between glass and the individual liquids are seen in Figure 6. So the contact angle seems to be one of the key factors of the capillary action, so that should be important in the follow-up studies.

The fillings of the hollow fibers are performed as is written in Materials and test methods. Every resin component and curing agent was examined by the filling of five fibers. The fibers sucked the resin droplet, which was placed to the end of the fibers. Average speed was calculated by the necessary time to cover a section (Figure 7).

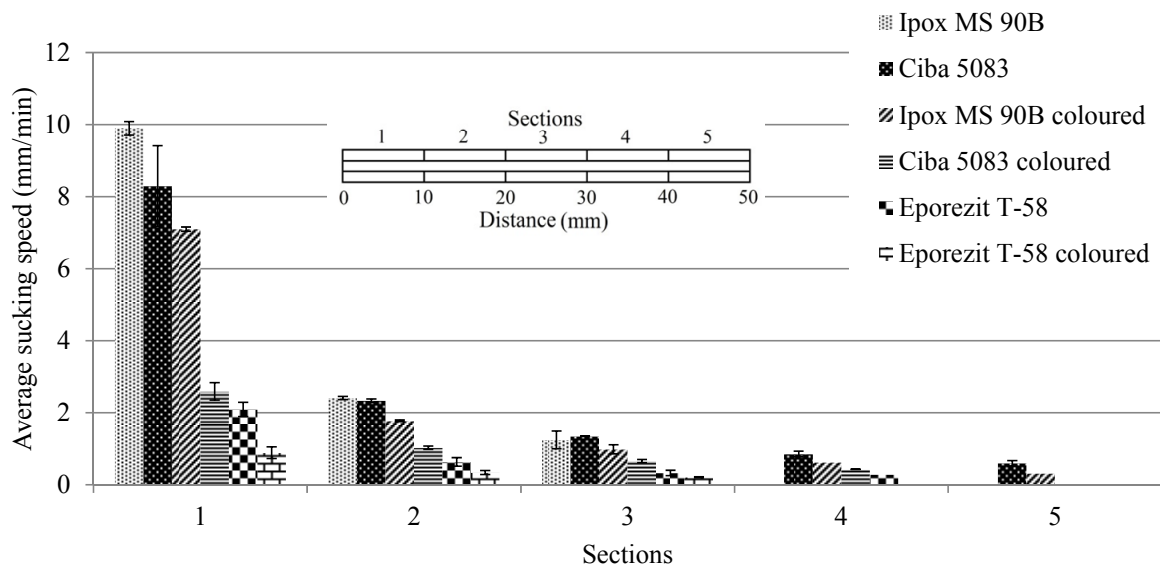


Figure 7. The average speed of the curing agents in the function of the sections

In Figure 7 it is seen, that deceleration was observed at the filling of the hollow fibers with both the resin component and the curing agent, and the decelerating mode is similar. In some cases the liquids stopped due to the liquid friction before it reached the end of the fiber. In summary it can be reported, that the colouring slowed down the speed of the liquids in the hollow fibers, consequently the higher viscosity means lower filling speed, as it is seen in Figure 9.

The speed of the individual liquids also depends on the contact angle between them and glass. On the dependence of contact angles (Figure 6) the speed of sucking shows a tendency of slowing down (Figure 8).

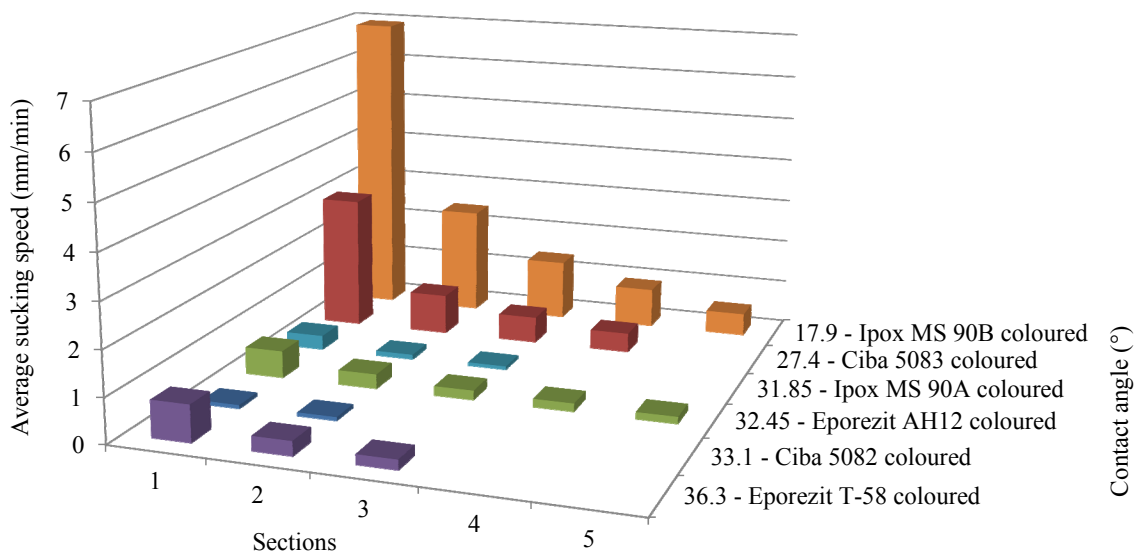


Figure 8. The speed of the coloured liquids in the function of the contact angle at each section

In Figure 8 it can be seen, that the lower is the contact angle between the materials the better is the wetting of the surface, so the capillary effect fills the fiber faster. There was also a slowing tendency in the sucking speed as a function of the viscosity (Figure 9).

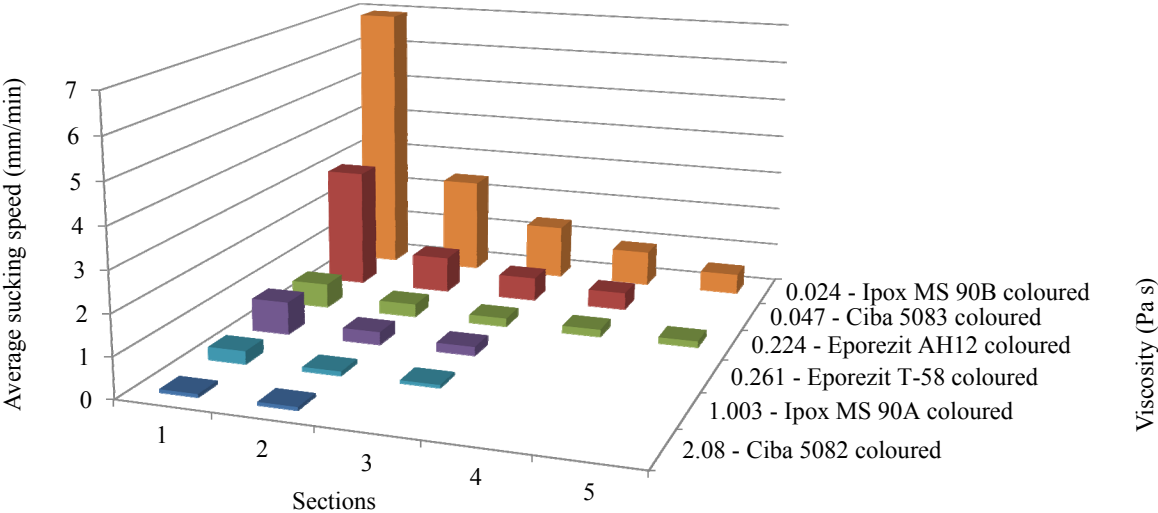


Figure 9. The speed of the coloured liquids as a function of the viscosity

The shearing rate in the fibers during filling was calculated by Equation 3, and the viscosity related to shear rate was read from results of the viscosity vs. shear rate function of the rheological measurements. Regarding Figure 9 it is seen, that the filling speed depends a lot on the viscosity of the liquid. In Figure 8 and in Figure 9 the speed of the same liquids is shown, the difference is ordering by the contact angle or by the viscosity. Viscosity shows a stronger effect on the sucking speed, which is also written in the capillary height equation [30].

Summary

Hollow and solid fibers have been compared as reinforcements. The tensile strength of the fibers was determined, and it was shown that the tensile strength changes inversely with FCF. The tensile strength of the hollow fibers is 85% higher, and the Young modulus is 64% higher than that of the solid fibers. The bending modulus of the fibers have been defined, and the bending modulus of the hollow fibers seemed to be 45% higher than that of the solid fibers, owing to the higher ratio of lower mass and moment of inertia related to the cross sectional

area. The filling ability of the hollow fibers was examined by liquids, and it was shown that there is a relation between contact angle, viscosity and the filling speed made by the capillary action.

Further work to be devoted to the preparation of composite plates reinforced with hollow fibers, and to the examination of the mechanical properties of the composite plates. The filling of the hollow fibers in composites with different liquids is planned, filling them both with healing agent and with indicator liquids, which shows if the structure is damaged.

Acknowledgements

This work is connected to the scientific program of the "Development of quality-oriented and harmonized R+D+I strategy and functional model at BME" project. This project is supported by the New Széchenyi Plan (Project ID: TÁMOP-4.2.1/B-09/1/KMR-2010-0002).

The work reported in this paper has been developed in the framework of the project "Talent care and cultivation in the scientific workshops of BME" project. This project is supported by the grant TÁMOP - 4.2.2.B-10/1--2010-0009.

One of the authors, Sándor Kling, would like to give thanks to Professor Ian Bond (University of Bristol, United Kingdom) for giving useful hints and experiences in the project.

References

1. Chawla KK. *Composite materials: science and engineering*. Birmingham: Springer Science, 1998.
2. Deák T and Czigány T. Chemical composition and mechanical properties of basalt and glass fibers: A comparison. *Text Res J*. 2009; 79: 645-51.
3. Jung I, Kim SY and Oh TH. Effects of Spinning Conditions on Shape Changes of Trilobal-shaped Fibers. *Text Res J*. 2010; 80: 12-8.
4. Hinüber C, Häussler L, Vogel R, Brünig H, Heinrich G and Werner C. Hollow fibers made from a poly(3-hydroxybutyrate)/poly- ϵ -caprolactone blend. *Express Polym Lett*. 2011; 5: 643-52.
5. Dhanalakshmi M and Jog JP. Preparation and characterization of electrospun fibers of Nylon 11. *Express Polym Lett*. 2008; 2: 540-5.
6. Shibulal GS and Naskar K. Exploring a novel multifunctional agent to improve the dispersion of short aramid fiber in polymer matrix. *Express Polym Lett*. 2012; 6: 329-44.
7. Kim TJ and Park CK. Flexural and tensile strength developments of various shape carbon fiber-reinforced lightweight cementitious composites. *Cement Concrete Res*. 1998; 28: 955-60.
8. Park SJ, Seo MK and Shim HB. Effect of fiber shapes on physical characteristics of non-circular carbon fibers-reinforced composites. *Mat Sci Eng A-Struct*. 2003; 352: 34-9.
9. Beyerlein IJ, Zhu YT and Mahesh S. On the influence of fiber shape in bone-shaped short-fiber composites. *Compos Sci Technol*. 2001; 61: 1341-57.
10. Bond I, Hucker M, Weaver P, Bleay S and Haq S. Mechanical behaviour of circular and triangular glass fibres and their composites. *Compos Sci Technol*. 2002; 62: 1051-61.

11. Rosen W, Kettler E and Hashin Z. *Hollow glass fibre reinforced plastics*. Philadelphia: General Electric Missile & Space Division, 1962, p.157.
12. Dry C. Matrix cracking repair and filling using active and passive modes for smart timed release of chemicals from fibers into cement matrices. *Smart Mater Struct*. 1994; 3: 118-23.
13. Noland R and O'Brien T. Hollow carbon fibers. Patent US5338605, USA, 1994.
14. Jensen T. Hollow glass fiber bushing, method of making hollow fibers and the hollow glass fibers made by that method. Patent US4758259, USA, 1988.
15. Ferguson J. Carbon fibers. Patent US6242093, USA, 2001.
16. Hucker MJ, Bond IP, Haq S, Bleay S and Foreman A. Influence of manufacturing parameters on the tensile strengths of hollow and solid glass fibres. *J Mater Sci*. 2002; 37: 309-15.
17. Yang X, Wang R and Fane AG. Novel designs for improving the performance of hollow fiber membrane distillation modules. *J Membrane Sci*. 2011; 384: 52-62.
18. Koonaphapdeelert S, Wu Z and Li K. Carbon dioxide stripping in ceramic hollow fibre membrane contactors. *Chem Eng Sci*. 2009; 64: 1-8.
19. Pang J and Bond I. 'Bleeding composites'--damage detection and self-repair using a biomimetic approach. *Compos Part A-Appl S*. 2005; 36: 183-8.
20. Pang J and Bond I. A hollow fibre reinforced polymer composite encompassing self-healing and enhanced damage visibility. *Compos Sci and Technol*. 2005; 65: 1791-9.
21. Trask R, Williams G and Bond I. Bioinspired self-healing of advanced composite structures using glass hollow fibres. *Journal of the Royal Society Interface*. 2007; 4: 363-71.
22. Trask RS and Bond IP. Biomimetic self-healing of advanced composite structures using hollow glass fibres. *Smart Mater Struct*. 2006; 15: 704.
23. Zhang M and Rong M. *Self-healing polymers and polymer composites*. Hoboken: John Wiley & Sons, Inc., 2011.
24. EN ISO 5079. Determination of braking force and elongation at break of individual fibres.
25. Potluri P, Atkinson J and Porat I. Large deformation modelling of flexible materials. *J Text Inst*. 1996; 87: 129-51.
26. Holden J. On the finite deflections of thin beams. *Int J Solids Struct*. 1972; 8: 1051-5.
27. Darby R. *Chemical engineering fluid mechanics*. New York: CRD Press, 2001.
28. Weibull W. A statistical distribution of wide applicability. *Journal of Applied Mechanics*. 1951; 18: 293-7.
29. Gupta P. Glass fibers for composite materials. In: Bunsell AR, (ed.). *Fibre reinforcements for composite materials*. New York: Elsevier, 1988, p. 19-71.
30. Kundu PK and Cohen IM. *Fluid Mechanics*. 4 ed. San Diego: Elsevier Science and Technology Books, 2008.